Historical warming reduced due to enhanced land carbon uptake

Elena Shevliakova[a], Ronald J. Stouffer[b], Sergey Malyshev[a], John P. Krasting[b], George C. Hurtt[c], and Stephen W. Pacala[a,1]

[a]Department of Ecology and Evolutionary Biology, Princeton University, Princeton, NJ 08544; [b]Geophysical Fluid Dynamics Laboratory, National Oceanic and Atmospheric Administration, Princeton, NJ 08540; and [c]Department of Geographical Sciences, University of Maryland, College Park, MD 20742

Contributed by Stephen W. Pacala, August 13, 2013 (sent for review December 3, 2012)

Previous studies have demonstrated the importance of enhanced vegetation growth under future elevated atmospheric CO_2 for 21st century climate warming. Surprisingly no study has completed an analogous assessment for the historical period, during which emissions of greenhouse gases increased rapidly and land-use changes (LUC) dramatically altered terrestrial carbon sources and sinks. Using the Geophysical Fluid Dynamics Laboratory comprehensive Earth System Model ESM2G and a reconstruction of the LUC, we estimate that enhanced vegetation growth has lowered the historical atmospheric CO_2 concentration by 85 ppm, avoiding an additional 0.31 ± 0.06 °C warming. We demonstrate that without enhanced vegetation growth the total residual terrestrial carbon flux (i.e., the net land flux minus LUC flux) would be a source of 65–82 Gt of carbon (GtC) to atmosphere instead of the historical residual carbon sink of 186–192 GtC, a carbon saving of 251–274 GtC.

climate change | carbon sink | earth system modeling

From the preindustrial times to present day, the total cumulative land carbon flux is estimated to be a source of 11 ± 47 Gt of carbon (GtC) to the atmosphere (1). The total historical direct land-use changes (LUC) carbon flux (i.e., only from anthropogenic activities without any effects of environmental change) is estimated at ∼160 GtC (2) with an uncertainty range of ±50% (1). The difference between the former and the latter implies a substantial residual terrestrial carbon sink. According to previous studies, the land was a carbon source to the atmosphere from the preindustrial period to the 1940s (3) and then became a carbon sink, which has steadily increased over the last 50 y (4, 5). For the 1980s and the 1990s the residual terrestrial carbon sink is estimated to be between −3.4 and 0.2 GtC/y and −4.2 and −0.9 GtC/y, respectively (6). One of the leading causes of the increasing residual terrestrial sink is believed to be enhanced vegetation growth under elevated levels of atmospheric CO_2 (i.e., CO_2 fertilization) (4, 6–9).

Previous studies have evaluated the implications of enhanced vegetation growth under future elevated atmospheric CO_2 for 21st century climate warming (10–12). Estimating the impact of enhanced vegetation growth on historical, transient climate change is surprisingly difficult: it cannot be simply deduced from the published idealized relationships such as an equilibrium climate sensitivity (13) or the Transient Climate Response to cumulative carbon Emissions (TCRE) (14). For example, analysis of simulations from the Coupled Climate Carbon Cycle Model Intercomparison Project (C4MIP) indicated that the TCRE is not constant from 1900 to 2000 (14). The TCRE does not include effects of any other greenhouse gases (GHGs), aerosols, or changes in historical forcings. The transient rate of temperature increase (15) and strengths of carbon sources and sinks (16, 17) both depend on the rate of change in the atmospheric CO_2 concentration. Moreover, feedbacks among climate, atmospheric CO_2, and land and ocean carbon exchanges must be accounted for in isolating the effect of any one factor. To assess the contribution of enhanced land carbon uptake to historical global warming requires a climate–carbon cycle model (i.e., an Earth System Model, ESM), capable of prognostically simulating the transient physical climate, and the exchanges of CO_2 among land, ocean, and atmosphere, as well as feedbacks between the climate and carbon system. The ESM must be forced by historical fossil fuel emissions and include an internally consistent treatment of historical LUC carbon emissions from agricultural conversion, wood harvesting, and regrowth of the previously used or logged (i.e., secondary) lands. Finally, the assessment needs to isolate the temperature change due to a particular process and show that its impact is significant relative to unforced climate variability.

Despite the fact that a number of comprehensive ESMs have been developed and analyzed during the last decade, most previous studies have not simulated historical LUC carbon fluxes in an internally consistent manner. For example, C4MIP (18) prescribed (rather than predicted) LUC CO_2 emissions for both agricultural conversion and logging from a regional bookkeeping model (2) although all land was modeled as unmanaged (i.e., without LUC) when computing land–atmosphere carbon fluxes. With the exception of one recent ESM analysis (ref. 19, with prescribed atmospheric CO_2), most ESM studies (e.g., refs. 14, 18) have not included land cover properties or carbon fluxes on secondary lands from forestry, which currently cover ∼30 million km^2. Such omission is likely to underestimate the net LUC emissions by 25–35% (20). A previous study with the stand-alone land component (21) of the Geophysical Fluid Dynamics Laboratory (GFDL) comprehensive ESM estimated an LUC carbon source of 45 GtC from wood harvesting and shifting cultivation during the 20th century.

Results

Experimental Design. In this study we address these challenges and quantify the climate benefit of enhanced terrestrial carbon uptake in reducing historical global warming. ESM2G is a comprehensive

Significance

This article provides estimates of the climate benefits due to CO_2 fertilization of the terrestrial biosphere. Without these benefits, the atmospheric CO_2 concentration would have risen by ∼200 ppm since the preindustrial period instead of the observed ∼115 ppm (an 80% increase), and the global climate would have warmed by an additional 0.31 ± 0.06 °C (a 40% increase). These findings were obtained with a National Oceanic and Atmospheric Administration/Geophysical Fluid Dynamics Laboratory comprehensive Earth System Model ESM2G.

Author contributions: E.S. and S.W.P. designed research; E.S. performed research; E.S., R.J.S., S.M., J.P.K., and G.C.H. contributed new analytic tools; J.P.K. performed the ESM2G model simulations; G.C.H. contributed historical land-use change reconstructions; E.S. analyzed data; and E.S., R.J.S., and S.W.P. wrote the paper.

The authors declare no conflict of interest.

Freely available online through the PNAS open access option.

[1]To whom correspondence should be addressed. E-mail: pacala@princeton.edu.

www.pnas.org/cgi/doi/10.1073/pnas.1314047110

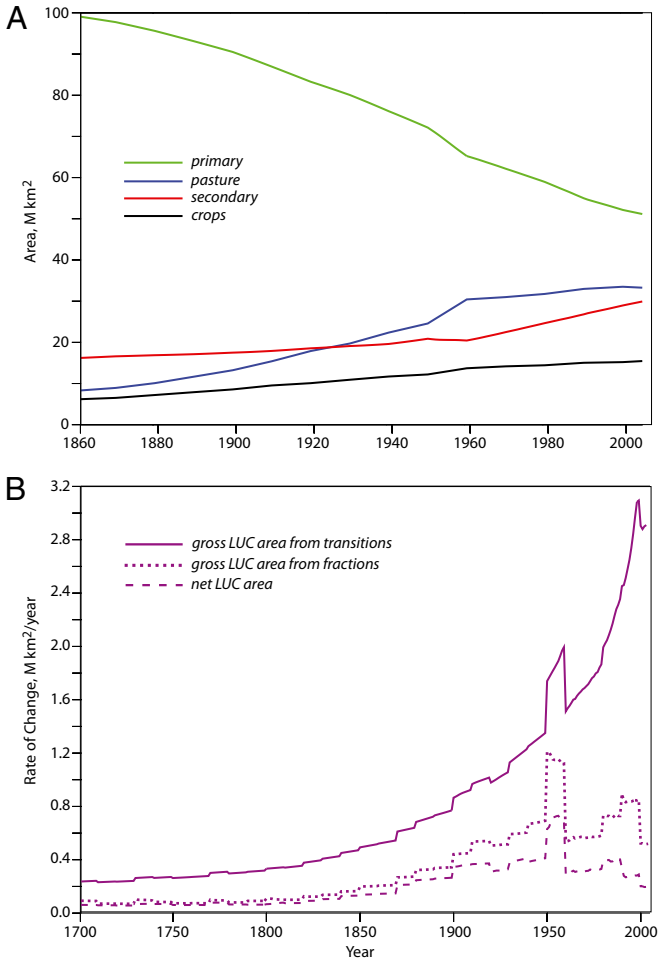

Fig. 1. (*A*) Global area [million (M) km^2] of croplands, pastures, secondary and primary lands in the historical reconstruction (23). (*B*) Net rate (dashed line, Mkm^2/y) and gross rate (solid line, Mkm^2/y) of area experiencing LUCs in the historical reconstructions (23) and used in the ESM2G experiments (computed from transitions rates from ref. 23). The dotted line (Mkm^2/y) shows gross rate of area under LUCs if one would use fractions instead of transitions rates to compute the gross rate. Secondary vegetation harvesting (represented by secondary to secondary transitions) is the major contributor to the difference between the solid and the dotted lines.

ESM (22) (*Methods*) that simulates effects of agricultural conversion, wood harvesting, and shifting cultivation. ESM2G uses an LUC (23) reconstruction from 1700 to 2005 (Fig. 1*A*), developed for use in the Coupled Model Intercomparison Project phase 5 (CMIP5, ref. 24). This reconstruction specifies gridded transitions rates among croplands, pastures, secondary (i.e., recovering after logging or abandonment), and primary (i.e., unmanaged) lands (Fig. 1*B*). ESM2G simulates both effects of changes in land physical characteristics on climate and the associated carbon fluxes on managed and unmanaged lands (i.e., LUC C fluxes), which in turn respond to changes in physical climate and atmospheric CO_2 concentration.

We conducted three types of CO_2 emissions-driven experiments from 1861 to 2005: historical (EH), historical without LUC (EHnoLU), and historical without the CO_2 fertilization effect on vegetation (EHnoFR). The historical changes in solar, volcanic, GHGs (other than CO_2), and aerosols forcings were prescribed in all experiments based on CMIP5 (24) recommendations. To separate the signal of the specific processes from unforced climate variability, each experiment type included three ensemble members. In all experiments atmospheric CO_2 concentrations and climate were predicted by ESM2G. The EH and EHnoFR experiments used the historical LUC reconstruction whereas EHnoLU experiments assumed that all lands remained in an unmanaged (i.e., primary) state. In the EH and EHnoLU experiments, vegetation was allowed to experience enhanced growth from the increasing levels of atmospheric CO_2. In the EHnoFR experiments vegetation growth and resultant changes in soil carbon were simulated as if the atmospheric CO_2 concentration had remained at the preindustrial level of 286 ppm (with the same LUC reconstruction) whereas the physical climate system did respond to increasing levels of atmospheric CO_2.

To estimate the carbon flux caused only by LUC in the absence of changes in climate and atmospheric CO_2 (i.e., the "direct" LUC flux, as in the bookkeeping estimate, ref.2), we conducted a fourth type of experiment (CLUonly). CLUonly experiments were conducted with prescribed preindustrial radiative forcings, including atmospheric CO_2 concentration (i.e., 286 ppm), using the same historical reconstruction of LUC as the EH and EHnoFR experiments. The direct LUC carbon flux is then used to compute residual fluxes (i.e., the net land C flux minus LUC C flux) from the EH and EHnoFR experiments, similar to the carbon budgeting approaches in the literature (e.g., ref. 6).

Land Carbon Uptake, Historical Changes in Atmospheric CO_2 and Temperature. The EH experiments capture the observed warming trend of the 20th century and the observed atmospheric CO_2 concentration increase (Figs. 2 and 3*B*), although the model has a small overestimate of 13 ppm in the 1950s. By 2005 the ensemble-mean atmospheric CO_2 concentration in the EH experiments is 388.3 ppm, ~8.5 ppm higher than the observed value of 379.8 ppm (www.esrl.noaa.gov/gmd/ccgg/trends/). In the EH experiments the switch from land carbon source to land carbon sink (Fig. 3*C*) occurs in the 1960s, approximately two decades later than in the observationally based estimate (3). This delay and the associated overestimate of the atmospheric CO_2 concentration in the EH experiments is likely due to a bias in the land-use reconstruction around the 1950s (Fig. 1*B*). In the LUC scenario (23) the rate of conversion from natural and secondary vegetation to pasture in the 1950s is implausibly almost twice the

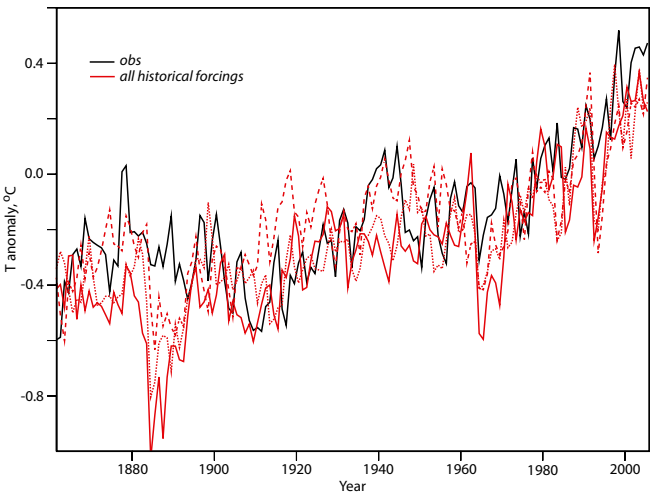

Fig. 2. Annual averaged surface air temperature anomaly (°C) simulated by three ensemble members of EH experiment (red lines). The observed (black line) is from the Climatic Research Unit, University of East Anglia HADCRUT3 dataset (www.cru.uea.ac.uk/cru/data/temperature). Temperature anomalies are computed against the 1961–1990 mean for the same locations as in HADCRUT3 dataset with the atmospheric reference temperature over the land and sea surface temperature for the oceans (note that the number of observations is changing through time in HADCRUT3).

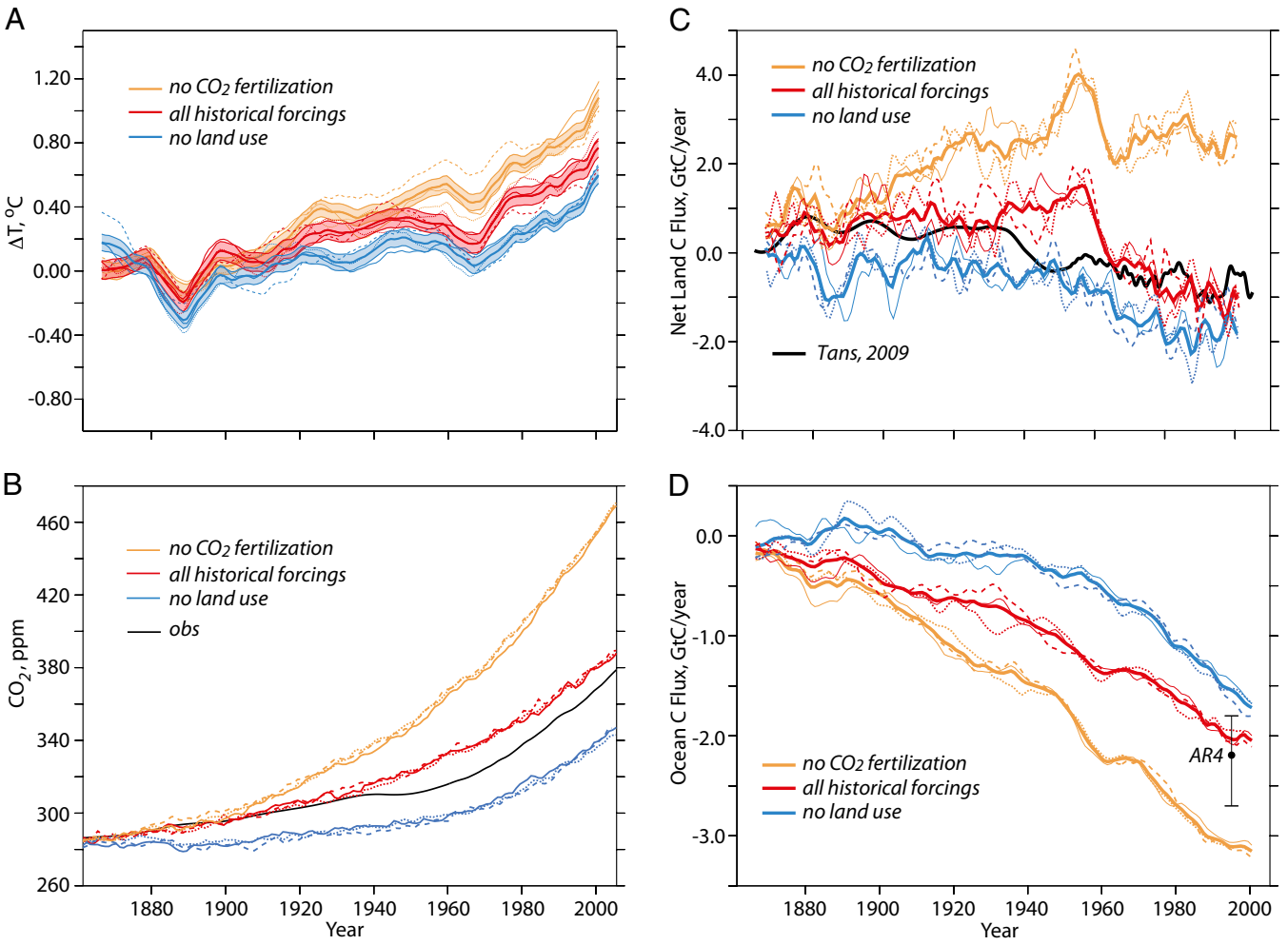

Fig. 3. (*A*) Change in annual, globally averaged surface air temperature (10-y smoothed, °C, ensemble mean) simulated in the emission-driven ESM2G experiments from preindustrial to current under all historical forcings (thick red line, EH), without LUCs (thick blue, EHnoLU), and without enhanced growth effect (orange, EHnoFR). The shading represents decadal variability (2 × SD) computed from the 400 y of the control simulations. The thin and two dashed lines represent each ensemble realization (10-y smoothed). (*B*) Annual atmospheric (mass-weighted), globally averaged CO_2 concentrations (ppm) simulated by three ensemble members of EH (red lines), EHnoLU (blue lines), and EHnoFR (orange lines) experiments. The black line is the observed atmospheric CO_2 concentration (www.esrl.noaa.gov/gmd/ccgg/trends). Net land (*C*) and ocean (*D*) carbon fluxes (10-y smoothed) simulated by three ensemble members of EH (red lines), EHnoLU (blue lines), and EHnoFR (orange lines) experiments. The *y*-axis scale is different in *C* and *D*. The black line in *C* is the observations-based reconstruction (3). The black bar in *D* is an estimate in ref. 6.

value in the preceding or in the following decade: 5.4×10^5 km^2/y in the 1940s, 9.4×10^5 km^2/y in the 1950s, and 4.8×10^5 km^2/y in the 1960s. The rate of conversion to croplands is also substantially higher in the 1950s: 1.8×10^5 km^2/y in the 1940s, 2.9×10^5 km^2/y in the 1950s, and 1.9×10^5 km^2/y in the 1960s. In the ESM2G model conversion of natural and secondary lands to pasture and croplands entails clearing of vegetation and release of carbon into the atmosphere.

The difference between EH and EHnoLU experiments quantifies the combined biogeochemical (e.g., emission of CO_2 to atmosphere) and biophysical (e.g., influence of changes in land properties on energy and moisture fluxes) effects of LUC on temperature (Fig. 3*A*). By 2005 in the EH experiments, the historical LUC elevates the atmospheric CO_2 concentration by ~43 ppm compared with the EHnoLU experiment (Fig. 3*B*). For the 1995–2005 period, the warming is 0.17 ± 0.06 °C larger in the EH ensemble mean than in the EHnoLU ensemble mean, where the 0.06 °C uncertainty range is $\sqrt{2}$ times the SD of decadal variability in the preindustrial control simulation (0.04 °C).

The enhancement of vegetation growth under elevated CO_2 levels is critical to the dynamics of terrestrial biosphere sources and sinks in the 20th century. In the EHnoFR experiment the atmospheric CO_2 concentration reached 472 ppm by 2005, almost 92 ppm higher than the observed level of 379.9 ppm, and 85 ppm higher than the 2005 level in the EH simulation. Whereas the atmospheric CO_2 concentration increased almost twice as much in the EHnoFR experiments compared to the EH experiments, the ocean C uptake increased by ~50% from −2.1 to −3.2 GtC/y (Fig. 3*D*). If ocean uptake in the EHnoFR experiments had remained the same as in the EH experiments, then the atmospheric CO_2 concentration would have been ~130 ppm higher. In the EHnoLU experiments the ocean C uptake decreased to −1.7 GtC/y, highlighting the relationship between oceanic carbon uptake and atmospheric CO_2 concentration.

LUC and Residual Land Fluxes. The total residual terrestrial carbon flux is defined as a difference between the net land and direct LUC carbon fluxes. It is widely used in carbon budgeting analyses to characterize the strength of land sources and sinks. An

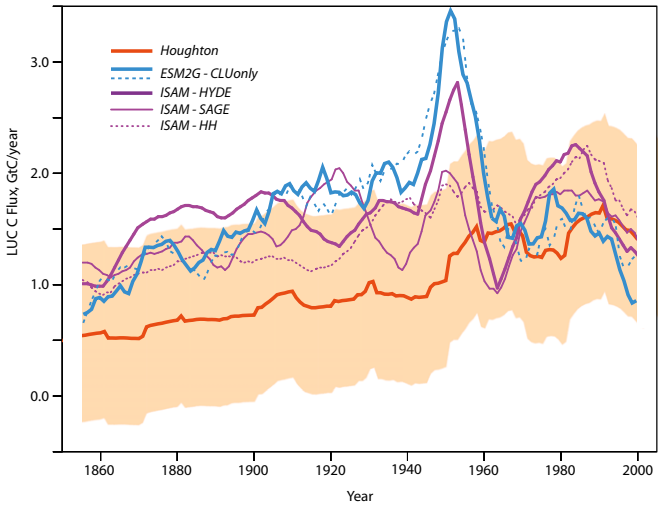

Fig. 4. Comparison of the direct land-use flux from the ESM2G CLUonly experiments with historical reconstruction of LUC (23) (blue solid and dashed lines, 10-y running mean), the ISAM model with three different scenarios of LUC change (25) (purple lines, 10-y running mean), and the bookkeeping model (2) (brown line; the shading is the uncertainty range). Note that the forest growth curves used in the bookkeeping method (2) are based on contemporary data and the current LUC fluxes in (2) reflect the current CO_2 and climate effects on the regrowing forests. A positive carbon flux is a source to atmosphere from land.

ESM historical simulation with a larger direct LUC C source (a positive flux into atmosphere) requires a larger residual C sink (a negative flux into atmosphere) to obtain the same net land C flux. From 1860 to 1949 the CLUonly experiments simulate a cumulative direct LUC flux of 128 GtC, a value 83% higher than the estimate of 70 GtC from the bookkeeping model (2) (Fig. 4, brown line). However, during this period, the CLUonly cumulative LUC flux agrees well with the recent estimate of 112–137 GtC obtained with the Integrated Science Assessment Model (ISAM) (25), which includes agricultural conversion and wood harvesting (Fig. 4, purple line). From the 1940s to 1960s, the direct LUC fluxes from ESM2G are higher than those from the bookkeeping method estimates (2), but values from the ESM2G simulations and from the bookkeeping method are similar after 1960 (Fig. 4). Furthermore, the LUC reconstruction (23) has higher rates of LUC for the tropics before the 1960s than those in the bookkeeping method (2).

After the 1960s, ESM2G, ISAM (25), and the bookkeeping method (2) use reconstructions based on the Food and Agriculture Organization (FAO) records. Before the 1960s LUC histories are more uncertain because reconstructions rely on the empirical approaches such as scaling the rate of agricultural conversion for cropland and pasture as well as wood harvesting as a function of population. In Fig. 4, throughout the entire period from 1861 to 2005 we used the uncertainty range of ±0.8 GtC/y reported in ref. 2 for the 1980s and the 1990s. It is likely that that the uncertainty is considerably larger before 1960s, before the availability of the FAO records.

Because the LUC reconstruction (23) consists of spatially gridded transition rates among land-use categories (not area fractions), which we applied starting in 1700, and because ESM2G represents subgrid land-use heterogeneity (22), ESM2G simulations with the LUC reconstruction (23) have a larger gross area (Fig. 1*B*) affected by land use than previous studies with comprehensive ESMs (19) imposing the same LUC reconstruction only after 1850 or lower-resolution models (12) representing only net changes in fractions of land-use categories and ignoring such processes as wood harvesting worldwide.

By differencing the net land carbon fluxes from the EH ensemble experiments and the LUC flux from CLUonly experiments, we estimate the 1861–2005 cumulative residual historical terrestrial C sink from −186 to −192 GtC. Similarly, by using the net land carbon fluxes from the EHnoFR ensemble experiments, we estimate the cumulative residual terrestrial C source from 65 to 82 GtC. These ranges represent spread due to unforced variability in the ESM2G ensemble experiments. The ranges do not reflect uncertainty in the LUC reconstructions or other sources of the ESM uncertainty. In the EH experiments the primary and secondary ensemble-mean terrestrial residual sinks are, respectively, −97 and −48 GtC from 1861 to 2005. The simulated historical terrestrial residual fluxes for the 1980s and 1990s are consistent with the published estimates (6) (Fig. 5). In the EHnoFR experiments carbon sinks decrease without the enhanced vegetation growth and the carbon sources are amplified by an additional warming. The difference between the terrestrial residual fluxes in EH and EHnoFR experiments is from 251 to 274 GtC due to internal climate variability.

Discussion

Comparison of EH Simulations with Other Estimates. Unlike the EHnoFR or EHnoLU experiments, the EH experiments with CO_2 fertilization are consistent with the observations of warming and atmospheric CO_2 concentrations (Fig. 3*B*) as well as with the inferred observational estimates of the net land and ocean carbon fluxes (Figs. 3 *C* and *D*). From 1861 to 2005 the total cumulative land ensemble-mean carbon flux was ∼42 GtC (a net source) in the EH experiment, which is in the range of the recently published estimate (1) of 11 ± 47 GtC. A large fraction (58%) of this simulated source is from the 1941–1960 period (24.5 GtC) when the LUC scenario may have a bias (Figs. 1*B* and 4), which itself may be related to the biases in the original pasture data (26).

The global cumulative net ensemble-mean LUC flux from 1860 to 2005 in the ESM2G EH experiments is 210 GtC. This value is higher than the best-guess bookkeeping model estimate in ref. 2 but is in the range of 210–230 GtC estimated by the stand-alone model ISAM forced by historical climate data and three different land-use reconstructions (25). ISAM accounted

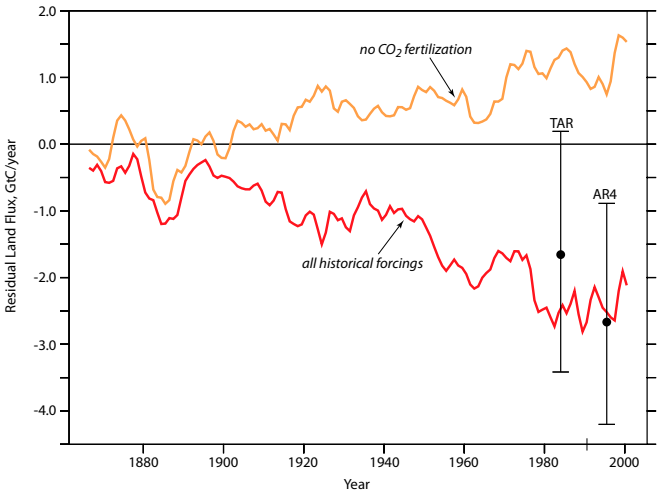

Fig. 5. Terrestrial residual (i.e., the net land flux minus LUC flux) carbon flux (GtC/year) from 1861 to 2005 for historical (EH) and "no CO_2 fertilization" (EHnoFR) experiments (ensemble means). The net land and LUC fluxes are from the corresponding ESM2G experiments. Negative values represent land carbon sinks and positive values represents land carbon sources. The black bars are estimates of terrestrial residual sinks from the revised third (TAR) and fourth (AR4) assessment reports of the Intergovernmental Panel on Climate Change, as reported in ref. 6.

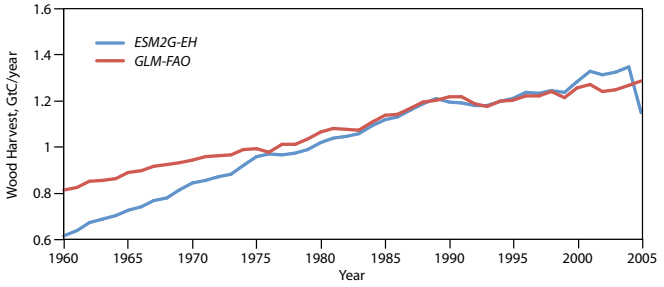

Fig. 6. Global wood harvest (GtC/y) as simulated by ESM2G in the EH experiments (blue line, an ensemble mean) and as estimated by the Global Landuse Model (GLM) from the FAO statistics in ref. 23. In the GLM estimate, FAO national wood harvest volume data for coniferous and nonconiferous round wood were multiplied by the harvest density values of 0.225 and 0.325 Mg C m^{-3}, respectively, to convert these national statistics to weight of carbon harvested (23).

for nitrogen–carbon cycling interactions on both natural and secondary lands. Furthermore, the simulated harvested wood biomass from the EH experiments compares well with the estimates derived from the FAO data (Fig. 6).

The estimated effect of the enhanced land carbon uptake due to CO_2 fertilization on the atmospheric CO_2 concentration and global temperature is large, whereas the magnitude of the CO_2 fertilization effect is consistent with other studies. For example, GPP in the EH experiments increased by 0.32 GtC/(y ppm) (24%) as atmospheric CO_2 increased from 286 ppm in the 1860s to 388.3 ppm by 2005 (35%) compared with 0.27 GtC/(y ppm) in ref. 27. Finally, to be compatible with the observed atmospheric CO_2 record, enhanced uptake must compensate for warming-induced sources or warming-reduced sinks. For example, in the EHnoFR experiments, GPP decreased over the historical period by 6%.

The ESM2G model is comparable in its complexity and in its behavior to other CMIP5 ESMs (e.g., ref. 28). We expect most CMIP5 ESMs to behave qualitatively similar to ESM2G in emission-driven experiments with historical LUC scenarios and without CO_2 fertilization. With an exception of a very few models (e.g., ref. 19), most models do not include representation of nitrogen cycling, nor do they include phosphorus cycling, soil microbial responses, acclimation of different plant species to increased temperatures, and peatland dynamics. The magnitude of the climate benefit of CO_2 fertilization in a particular ESM is likely to depend on the strength of CO_2 fertilization effect, nutrient-availability feedbacks (e.g., nitrogen and phosphorus), transient climate sensitivity, and on its LUC implementation and scenarios. All of these are uncertain, in particular, land use reconstructions before the 1960s. Because a large fraction of CO_2 emissions remains in the atmosphere, the CO_2 released from LUC in the first part of the 20th century is still contributing to ongoing warming. To better understand past, ongoing, and future changes in the terrestrial carbon cycling, uncertainty in both reconstructions of LUC and in ESMs' treatment of agricultural and forestry management needs to be characterized and reduced, particularly on the regional scale. Future studies using new kinds of ESM experiments need to explore how ESMs' structure, particularly their representation of CO_2 fertilization and down-regulation mechanisms, may affect the strength of the carbon uptake and at which levels of the atmospheric CO_2 concentrations CO_2 fertilization effect will cease.

Conclusion

The results of our study indicate that historical enhanced vegetation growth has avoided release of 251–274 GtC, about an additional 85 ppm of atmospheric CO_2 concentration, and a warming of 0.31 ± 0.06 °C. To accurately predict observed trends in both temperature and the atmospheric CO_2 concentration over the 20th century, ESMs need to account for the interaction of LUC and enhanced vegetation growth, including vegetation regrowth on the secondary lands. CO_2 fertilization is a plausible but debated mechanism for the ongoing land carbon sink. The empirical evidence for enhanced vegetation growth under elevated CO_2 remains equivocal (29–32). The model used here does not include nitrogen or phosphorus limitations on carbon uptake. Some modeling (33) and observational (34–36) studies have found that nitrogen availability has not significantly affected global carbon uptake over the 20th century, whereas others have reached the opposite conclusion (37). The magnitude and the sign of the future net land carbon flux will impact the atmospheric CO_2 growth rate, climate change, and any efforts to mitigate it. Because of the importance of the land sink in reconciling atmospheric CO_2 and climate records, this study adds urgency to independently test and isolate the mechanisms responsible for the growing terrestrial C sink.

Methods

For this study we used the GFDL coupled climate–carbon cycle model ESM2G (22), which can simulate atmospheric and oceanic climate, ecology, and biogeochemistry and their variability from the diurnal time scale through multicentury climate change. ESM2G uses the same atmospheric component as the GFDL physical climate model CM2.1 with revised land, sea ice, and iceberg components as well as terrestrial ecology and ocean biogeochemistry. For the ocean component, ESM2G uses Generalized Ocean Layer Dynamics (GOLD). Land model version 3 (LM3) is used to simulate interactively the vegetation distribution and functioning, including carbon cycling among vegetation, soil, and atmosphere (21). LM3 resolves subgrid land heterogeneity with respect to different land-use activities (21): each grid cell includes up to 15 different tiles to represent differences in above- and belowground hydrological and carbon states among croplands, pastures, natural, and secondary lands. In the ocean, Tracers for Ocean Phytoplankton with Allometric Zooplankton version 2.0 (TOPAZ 2.0) is used to represent carbon cycling. ESM2G has a resolution of ~2° for the atmosphere and land, ~1° for the ocean and sea ice, 24 vertical layers in the atmosphere, 50 vertical layers in the ocean, and 20 layers in the soil. In emission-driven experiments with LUC reconstruction, releases of the CO_2 from deforestation, land clearing, and agricultural activities entered into three anthropogenic pools with three different rates of turnover (1, 10, and 100). Emissions from these three pools then were exchanged with the atmosphere.

From an arbitrary set of initial conditions, the model was integrated over 1,000 model years with CO_2 restoring to 286 ppm to achieve equilibrium in both the physical climate and the carbon cycle. Once the model achieved equilibrium, the 500-y preindustrial control simulations with fixed 1860 radiative forcing and potential vegetation (i.e., primary lands) were initialized. Three ensemble simulations were performed with the model using time-varying historical LUC reconstruction from 1700 to 1860, fixed preindustrial radiative forcing, and atmospheric CO_2 concentration restored to 286 ppm. The EH and EHnoFR ensemble simulations started from the initial conditions for December 31, 1860 of the three ensembles. The EHnoLU ensemble simulations were initialized directly from the preindustrial control simulation at the same point in time as the EH and EHnoFR simulations (relative to the control run) to minimize the effects of long-timescale climate drift. We applied all time-evolving historic forcings beginning in year 1861.

In the EHnoFR the model kept track of two different CO_2 tracers, one for land biosphere where the annual average CO_2 concentration was restored toward 286 ppm using a 1-y time scale, and one in which CO_2 was balanced by exchanges between land, ocean, atmosphere, and fossil fuel emissions. The second CO_2 tracer was used in the ESM2G radiation module in the EHnoFR experiments. Furthermore, ESM2G treats carbon and water exchanges consistently in all experiments (e.g., does not compute stomatal conductance for CO_2 exchange differently from the one for transpiration).

In the CO_2-concentration driven CLUonly experiments the atmospheric CO_2 concentration is restored to the observed preindustrial value of 286 ppm with a 1-y relaxation time constant, thus allowing land and ocean biosphere to experience more realistic diurnal and seasonal CO_2 cycles. The LUC C fluxes in this experiment do not include influences of climate change from increases in the concentrations of GHGs, changes in the aerosol concentration, or volcanoes. However, they do include the influence of natural climate variability that is evident in the LUC time series of the two CLUonly ensemble members (Fig. 5).

ACKNOWLEDGMENTS. We thank J. M. Gregory, A. Jain, J. L. Russell, T. C. Knutson, and C. Raphael for comments on the manuscript. E.S., S.M., and S.W.P. acknowledge support in part from the National Oceanic and Atmospheric Administration (US Department of Commerce) Grant NA08OAR4320752, the US Department of Agriculture Grant 2011-67003-30373, and the Carbon Mitigation Initiative at Princeton University, sponsored by British Petroleum.

1. Arora VK, et al. (2011) Carbon emission limits required to satisfy future representative concentration pathways of greenhouse gases. *Geophys Res Lett* 38(5):L05805.
2. Houghton RA (2008) *TRENDS: A Compendium of Data on Global Change* (Carbon Dioxide Information Analysis Center, Oak Ridge National Laboratory, US Department of Energy, Oak Ridge, TN).
3. Tans PP (2009) An accounting of observed increase in oceanic and atmospheric CO_2 and an outlook for the future. *Oceanography (Wash DC)* 22(4):26–35.
4. Pan Y, et al. (2011) A large and persistent carbon sink in the world's forests. *Science* 333(6045):988–993.
5. Ballantyne AP, Alden CB, Miller JB, Tans PP, White JWC (2012) Increase in observed net carbon dioxide uptake by land and oceans during the past 50 years. *Nature* 488(7409):70–72.
6. Denman KL, et al. (2007) Couplings between changes in the climate system and biogeochemistry. *Climate Change 2007: The Physical Science Basis. Contribution of Working Group I to the Fourth Assessment Report of the Intergovernmental Panel on Climate Change*, eds Solomon S, et al. (Cambridge Univ Press, Cambridge, UK).
7. Kramer PJ (1981) Carbon dioxide concentration, photosynthesis and dry matter production. *BioScience* 31(1):29–33.
8. Prentice IC, Harrison SP, Bartlein PJ (2011) Global vegetation and terrestrial carbon cycle changes after the last ice age. *New Phytol* 189(4):988–998.
9. Lewis SL, et al. (2004) Concerted changes in tropical forest structure and dynamics: Evidence from 50 South American long-term plots. *Philos Trans R Soc Lond B Biol Sci* 359(1443):421–436.
10. Thompson SL, et al. (2004) Quantifying the effects of CO_2-fertilized vegetation on future global climate and carbon dynamics. *Geophys Res Lett* 31(23):L23211.
11. Matthews HD (2007) Implications of CO_2 fertilization for future climate change in a coupled climate–carbon model. *Glob Change Biol* 13:1068–1078.
12. Strassmann KM, Joos F, Fischer G (2008) Simulating effects of land use changes on carbon fluxes: Past contributions to atmospheric CO_2 increases and future commitments due to losses of terrestrial sink capacity. *Tellus B Chem Phys Meterol* 60(4): 583–603.
13. Manabe S, Wetherald RT (1967) Thermal equilibrium of the atmosphere with a given distribution of relative humidity. *J Atmos Sci* 24(3):241–259.
14. Matthews HD, Gillett NP, Stott PA, Zickfeld K (2009) The proportionality of global warming to cumulative carbon emissions. *Nature* 459(7248):829–832.
15. Stouffer RJ, Manabe S (1999) Response of a coupled ocean-atmosphere model to increasing atmospheric carbon dioxide: Sensitivity to the rate of increase. *J Clim* 12(8): 2224–2237.
16. Gregory JM, Jones CD, Cadule P, Friedlingstein P (2009) Quantifying carbon cycle feedbacks. *J Clim* 22(19):5232–5250.
17. Boer GL and Arora V (2009). Temperature and concentration feedbacks in the carbon cycle. *Geophys Res Lett* 36:L02704.
18. Friedlingstein P, et al. (2006) Climate-carbon cycle feedback analysis: Results from the C4MIP model intercomparison. *J Clim* 19:3337–3353.
19. Lawrence PJ, et al. (2012) Simulating the biogeochemical and biogeophysical impacts of transient land cover change and wood harvest in the Community Climate System Model (CCSM4) from 1850 to 2100. *J Clim* 25(9):3071–3095.
20. Houghton RA, et al. (2012) Carbon emissions from land use and land-cover change. *Biogeosciences* 9:5125–5142.
21. Shevliakova E, et al. (2009) Carbon cycling under 300 years of land use change: Importance of the secondary vegetation sink. *Global Biogeochem Cycles* 23(2):GB2022.
22. Dunne JP, et al. (2012) ESM2 global coupled climate-carbon Earth System Models Part II: Carbon system formulation and baseline simulation characteristics. *J Clim* 26: 2247–2267.
23. Hurtt GC, et al. (2011) Harmonization of land-use scenarios for the period 1500–2100: 600 years of global gridded annual land-use transitions, wood harvest, and resulting secondary lands. *Clim Change* 109(1):117–161.
24. Taylor KE, Stouffer RJ, Meehl GA (2012) An overview of CMIP5 and the experiment design. *Bull Am Meteorol Soc* 93(4):485.
25. Jain AK, Meiyappan P, Song Y, House JI (2013) CO_2 emissions from land-use change affected more by nitrogen cycle, than by the choice of land-cover data. *Glob Change Biol* 19(9):2893–2906.
26. Goldewijk KK (2001) Estimating global land use change over the past 300 years: The HYDE database. *Global Biogeochem Cycles* 15(2):417–433.
27. Arora VK, et al. (2009) The effect of terrestrial photosynthesis down regulation on the twentieth-century carbon budget simulated with the CCCma Earth System Model. *J Clim* 22:6066–6088.
28. Jones C, et al. (2013) 21st century compatible CO_2 emissions and airborne fraction simulated by CMIP5 Earth System models under 4 representative concentration pathways. *J Clim* 26:4398–4413.
29. Caspersen JP, et al. (2000) Contributions of land-use history to carbon accumulation in U.S. forests. *Science* 290(5494):1148–1151.
30. Phillips OL, Lewis SL, Baker TR, Chao KJ, Higuchi N (2008) The changing Amazon forest. *Philos Trans R Soc Lond B Biol Sci* 363(1498):1819–1827.
31. Gedalof Z, Berg AA (2010) Tree ring evidence for limited direct CO_2 fertilization of forests over the 20th century. *Global Biogeochem Cycles* 24(3):GB3027.
32. McMahon SM, Parker GG, Miller DR (2010) Evidence for a recent increase in forest growth. *Proc Natl Acad Sci USA* 107(8):3611–3615.
33. Jain A, et al. (2009) Nitrogen attenuation of terrestrial carbon cycle response to global environmental factors. *Global Biogeochem Cycles* 23:GB4028.
34. Barron AR, Purves DW, Hedin LO (2011) Facultative nitrogen fixation by canopy legumes in a lowland tropical forest. *Oecologia* 165(2):511–520.
35. Brookshire ENJ, Hedin LO, Newbold JD, Sigman DM, Jackson JK (2012) Sustained losses of bioavailable nitrogen from montane tropical forests. *Nat Geosci* 5(2): 123–126.
36. Norby RJ, Zak DR (2011) Ecological lessons from free-air CO_2 enrichment (FACE) 600 experiments. *Annu Rev Ecol Evol Syst* 42(1):181–203.
37. Thornton PE, Lamarque JF, Rosenbloom NA, Mahowald NM (2007) Influence of carbon-nitrogen cycle coupling on land model response to CO_2 fertilization and climate variability. *Global Biogeochem Cycles* 21(4):GB4018.